Lawrence Berkeley Laboratory
UNIVERSITY OF CALIFORNIA

Physics, Computer Science & Mathematics Division

Published in IEEE Transactions on Nuclear Science, Vol. NS-27, No. 1, February 1980. pp. 59-63

PERFORMANCE OF THE LEAD/LIQUID ARGON SHOWER COUNTER SYSTEM OF THE MARK II DETECTOR AT SPEAR

G. S. Abrams, C. A. Blocker, D. D. Briggs, W. C. Carithers, W. E. Dieterle, M. W. Eaton, A. J. Lankford, C. Y. Pang, E. N. Vella, M. Breidenbach, J. M. Dorfan, G. Hanson, D. G. Hitlin, P. Jenni and V. Lüth

May 1980

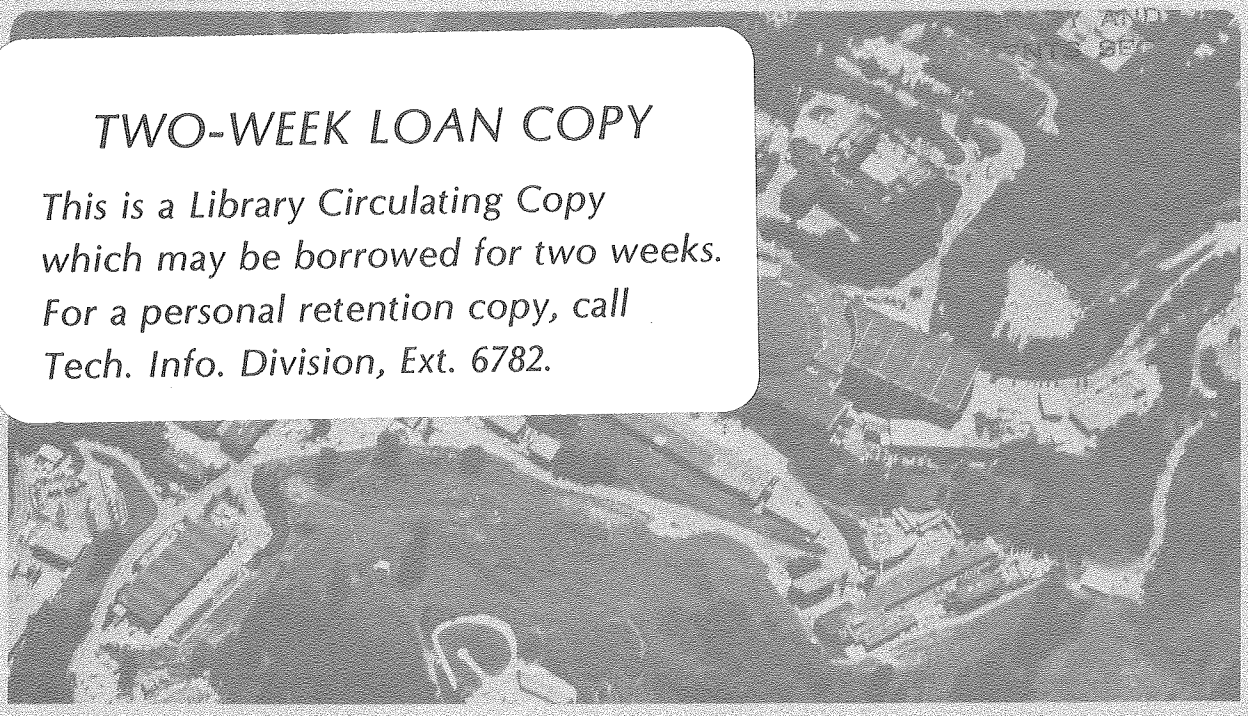

Prepared for the U.S. Department of Energy under Contract W-7405-ENG-48

DISCLAIMER

PERFORMANCE OF THE LEAD/LIQUID ARGON SHOWER COUNTER SYSTEM OF THE MARK II DETECTOR AT SPEAR

G. S. Abrams, C. A. Blocker, D. D. Briggs, W. C. Carithers, W. E. Dieterle,
M. W. Eaton, A. J. Lankford, C. Y. Pang and E. N. Vella
Lawrence Berkeley Laboratory
University of California, Berkeley, California 94720

and

M. Breidenbach, J. M. Dorfan, G. Hanson,
D. G. Hitlin, P. Jenni and V. Lüth
Stanford Linear Accelerator Center
Stanford University, Stanford, California 94305

The shower counter system of the SLAC-LBL Mark II detector is a large lead/liquid argon system of the type pioneered by Willis and Radeka[1]; however, it differs in most details and is much larger than other such detectors currently in operation. It contains, for example, 8000 liters of liquid argon and 3000 channels of low noise electronics, which is about eight times the size of the system of Willis et al.[2] in the CERN ISR. This paper reports, with little reference to design, on the operation and performance of the Mark II system during approximately a year and a half of operation at the Stanford Linear Accelerator Center's e^+-e^- facility, SPEAR. The design and construction of the system have previously been described[3] and a detailed discussion of all aspects -- design, construction, operation, and performance -- is in preparation.[4]

The Mark II Detector

The Mark II detector is a general purpose spectrometer for studying e^+-e^- collisions. The main components of the Mark II consist of a 5.0 kG solenoidal magnet, drift chambers for charged particle tracking, scintillators for time-of-flight information, lead/liquid argon shower counters, lead/proportional chamber endcap shower counters, and iron/proportional tube sandwiches for muon identification. The detector is shown in isometric view in Fig. 1.

The physics goals of the Mark II demand a shower counter system offering efficient detection of photons with energies from a few hundred MeV to several GeV, good energy resolution, very good angular resolution, good discrimination between electrons and hadrons, and good long-term stability. As an example of some of these physics demands, Fig. 2 shows an event of the sort

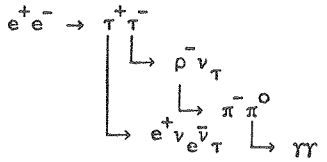

This event illustrates the power of the shower counter system, which is used here for positive identification of each detected particle -- e^+, π^-, and π^0. Fulfilling these requirements within the limited space between solenoidal magnet coil and iron flux return, and with a manageable electronic system, necessitated careful compromise in detector design.

General Design of Lead/Liquid Argon Shower Counters

The shower counter system consists of eight large ($1.5 \times 3.8 \times 0.3$ m^3) modules which cover 69% of polar angle θ and the full azimuthal angle φ except for 3° between each pair of modules. The internal structure ("stack") is composed of 37 planes of 2 mm antimony strengthened lead separated by 3 mm liquid argon gaps. This structure provides 20% energy deposit in liquid argon with 0.4 radiation length sampling and 14 radiation lengths depth overall for particles at normal incidence. Within the stack, large lead ground planes alternate with planes of lead strips oriented at 0° and 90° (3.8 cm wide) and 45° (5.4 cm wide). In order to reduce the number of electronics channels, many of these strips are ganged together in a manner which is a compromise between the demands of low energy photon efficiency and hadron/electron discrimination. An additional pair of 8 mm liquid argon gaps formed by "massless" 1.6 mm aluminum ground plates and strips are positioned in front of the stack to allow corrections to measured shower energy for radiative losses in the magnet coil. Altogether 1.5 radiation lengths of material precede the lead stack for particles at normal incidence.

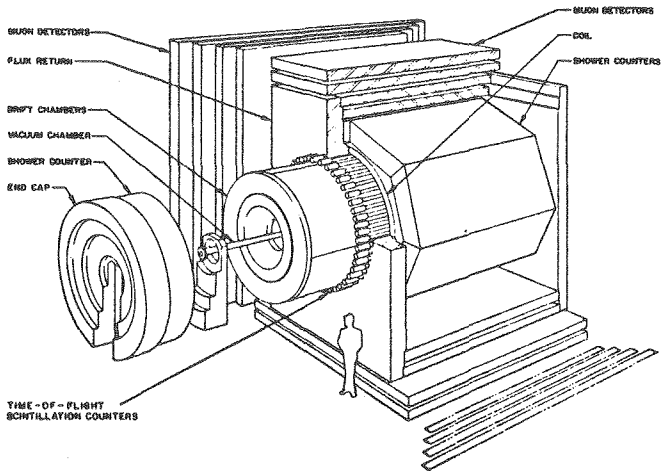

Fig. 1. Cutaway view of Mark II detector.

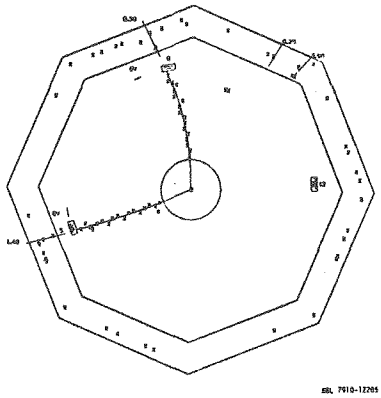

Fig. 2. Beam axis view of a reconstructed event of the sort $e^+e^- \rightarrow \tau^+\tau^- \rightarrow e^+\nu\nu + \rho^-\nu$ with the subsequent decays $\rho^- \rightarrow \pi^-\pi^0$ and $\pi^0 \rightarrow \gamma\gamma$.

Cryogenic Performance

Each of the eight shower counter modules is enclosed

in a welded aluminum box, and all modules are suspended in a common insulating vacuum vessel. Each module is refrigerated by liquid nitrogen heat exchangers welded to the aluminum box. To minimize thermal gradients in the lead stack, cool-down is performed with helium in the modules and takes approximately three days. After cool-down, liquid argon can be transferred into all modules in a few hours. After filling, liquid argon is not circulated, and the modules are connected to the storage dewar through the gas phase. With an insulating vacuum of 10^{-6} torr, heat loss is dominantly through transfer lines. Consumption of liquid nitrogen is 160 liters per hour during normal operation. Cool-down consumes about 50,000 liters.

The cryogenics for a many-thousand-liter liquid argon system which is inaccessible during normal operation requires extensive and redundant monitors of temperature, insulating vacuum, control valve positions, etc. for both the liquid argon and the liquid nitrogen refrigerant, as well as a failsafe control system based on good understanding of possible failure modes and environmental disruptions. The Mark II system has experienced no major problems during normal operation, although aspects of the emergency and interlock system have proven invaluable. The cryogenic problems encountered, broken ceramic insulators on cryo-temperature high voltage feedthroughs, damaged bellows in transfer lines due to stuck valve, and poisoning of liquid argon in storage dewar by liquid nitrogen leak from heat exchanger, have occurred during detector cool-down and transfer of liquid. Additionally, one fill of liquid argon (after the LN_2 leak) was discovered to be strongly poisoned by an extremely small concentration (too small for detection by analysis) of an unidentified electronegative impurity. Consequently, liquid argon is now tested in a small test chamber before transfer into the system.

The cryogenic system is large but manageable. It does require regular attention from the physicists on shift, as well as support from an experienced cryogenic technician on call.

Electronics Performance

The signal processing electronics consists of the detector strips and high voltage and calibration distribution within the liquid argon volume, charge sensitive preamplifiers and shaping amplifiers mounted on the detector module, and a sample-and-hold,[5] ADC, microprocessor system[6] in the control area. Measured equivalent noise charges (typically 9000 rms e^-) are consistent with estimates[1] of optimal noise for the chosen values of detector capacitance (typically 5 nF), high voltage blocking capacitance (6.25 nF), and bipolar filter time (220 ns). To exploit the small event rates during future operation at PEP, amplifier time constants are being lengthened to decrease both ballistic deficit and noise, yielding an improvement of approximately 2:1 in signal to noise. At PEP the electronics will provide a dynamic range of three orders of magnitude, from noise levels corresponding to less than 4 MeV incident energy to signals of over 4 GeV on individual channels.

Although all aspects of the electronics -- connections, amplifiers, shielding, sample-and-holds, calibration -- required extensive effort in design and set-up stages, the operation and performance of the electronics has been good. In particular, the electronics performance is satisfactory in the difficult high electromagnetic radiation environment of a bunched beam accelerator. To assure continued insensitivity to e-m fields at PEP, further attention is currently being given to shielding, grounding, and proper handling of instrumentation signals. The failure rate of electronics is low, less than two channels per week in a system of 3000 channels.

Physics Performance

The physics performance -- energy and angular resolutions, efficiencies, electron-hadron discrimination -- for the entire system of eight modules is consistent with expectations based on the chosen detector geometry and equal to or better than results obtained for a single module with a similar amount of preradiator in a test beam. Achieving this performance required considerable software development, which is discussed in subsequent sections.

Energy resolution for incident electrons has been measured using electrons of energy 1.5 to 3.7 GeV from Bhabha (elastic e^+-e^- scattering) events and using electrons of lower energy from photon conversions in the beam pipe. Typical energy spectra for 2.08 GeV Bhabhas and 125 - 175 MeV conversions are shown in Figs. 3 and 4. The

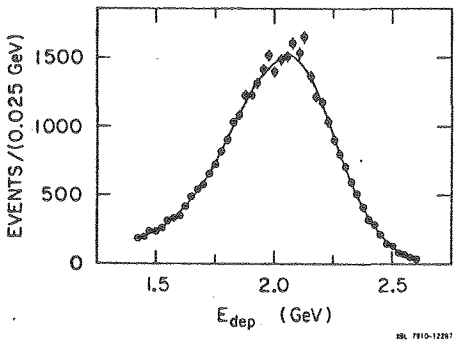

Fig. 3. Observed energy deposit for a sample of Bhabha electrons in all eight detector modules at beam energy of 2.08 GeV. The curve is the expected distribution assuming $\sigma/E = 11.6\%/\sqrt{E}$.

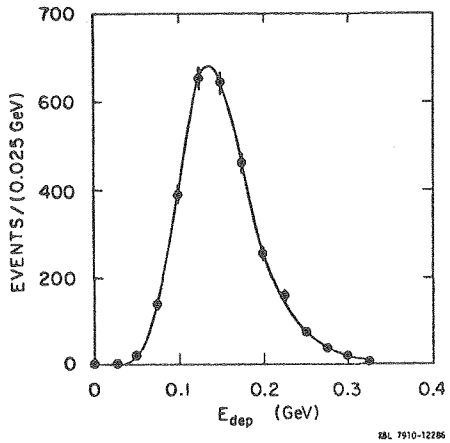

Fig. 4. Observed energy deposit for a sample of conversion electrons with momenta between 125 and 175 MeV/c. The curve is the expected distribution assuming $\sigma/E = 11\%/\sqrt{E}$.

energy resolution obtained for the system as a whole is $\sigma_e/E = 11.5\%/\sqrt{E}$ for electrons in the energy range from 200 MeV to 3.7 GeV. The energy resolution for photons has been measured, using photons of typically a few hundred MeV from ψ decays involving π^0's.

For photons which do not convert in the coil the resolution is $12\%/\sqrt{E}$, and for photons which do convert it is $13\%/\sqrt{E}$. Corrections for ionization and radiative losses in the coil, which will be discussed later, are necessary to achieve these resolutions.

Typical angular resolutions range from 3.6 mrads for high energy electrons to less than 8 mrads for low energy photons. These resolutions correspond to about

20% and 40% of the 38 mm width of a strip. For exclusive final states involving photons in the Mark II, very good angular resolutions allow precise fitting of events without need for extraordinary energy resolution. Figure 5 shows the fitted invariant mass of two photons from the decay $\psi' \to \psi\gamma\gamma$, an example in which a 5-C fit allows the measured photon energies to be essentially unused. The resulting rms width of the $\eta(548)$ peak is 1.5 MeV/c^2.

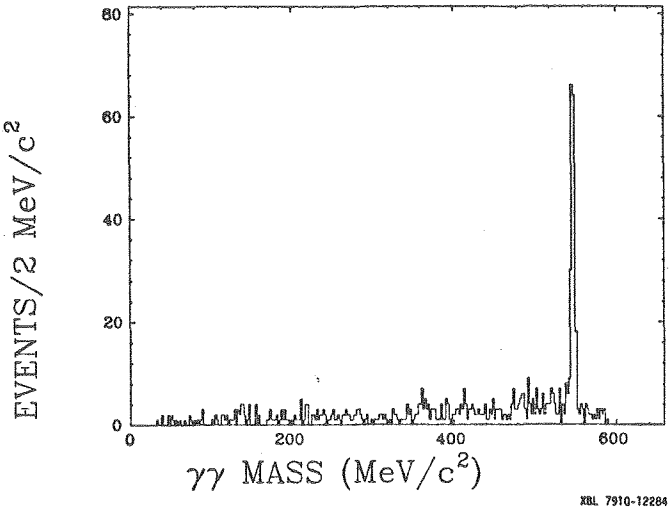

Fig. 5. $\gamma\gamma$ invariant mass distribution after 5-C fit to the reaction $\psi' \to \gamma\gamma\psi$, $\psi \to e^+e^-$. The rms width of η^o peak is 1.5 MeV/c^2.

The efficiency for photon detection has been determined by using the EGS[7] shower Monte Carlo to deposit energy according to the detector geometry and then reconstructing the photon using the normal analysis routines. The efficiency thus determined is checked using events of the sort $\psi \to \pi^+\pi^-\pi^o$. Detection of both charged pions and at least one of the decay photons of the pi-zero allows determination of the efficiency for detecting the second photon as a function of its energy. The results of these efficiency measurements are shown respectively as the solid curve and the data points in Fig. 6. Efficiency falls at low energies primarily for

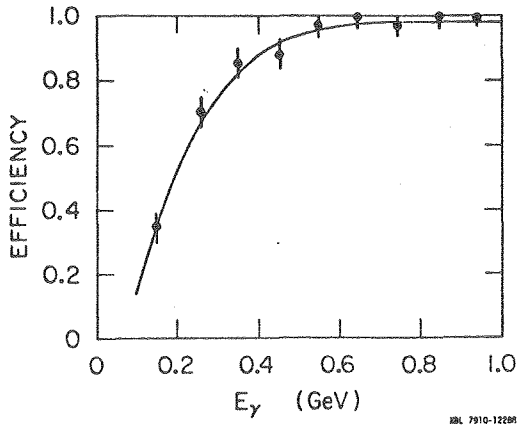

Fig. 6. Photon detection efficiency as a function of energy. Data points are measured values. The curve is a Monte-Carlo calculation.

three reasons: (1) low energy photons which interact in the 1.36 radiation length coil may deposit little energy in the lead stack, (2) shower fluctuations can cause little energy to appear in a given detector layer, and (3) noise fluctuations can reduce small signals below thresholds. The efficiency achieved is a compromise with the number of spurious hits reconstructed from noise fluctuations. This compromise is discussed in more detail in a later section. The efficiency shown in Fig. 6 for detection of individual photons translates into efficiencies for π^o and η^o detection shown in Fig. 7. These curves include solid angle coverage (64%) and branching ratios into photons.

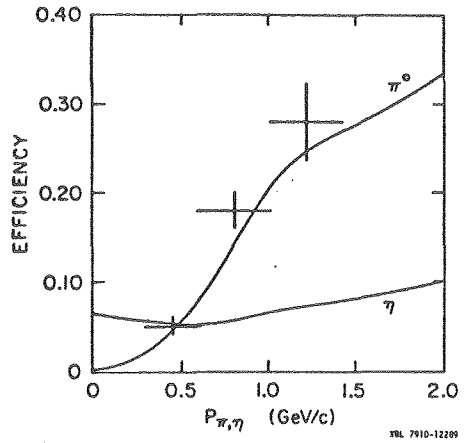

Fig. 7. π^o and η^o detection efficiencies as functions of momentum. Geometry (for seven detector modules) and branching fractions are included. Data points are measured π^o values. Curves are Monte-Carlo calculations based on photon efficiencies shown in Fig. 6.

The level of electron-hadron discrimination for particular physics applications can be chosen to provide the necessary combination of efficiency and rejection. Table 1 summarizes discrimination provided by a particular choice. For example, at 1.0 GeV electrons are identified with an 87% efficiency and a 1.5% probability of misidentifying a hadron as an electron. In

Table 1
Sample Electron-Hadron Discrimination

Momentum slice (GeV/c)	$P_{\pi\to\pi}$ (%)	$P_{\pi\to e}$ (%)	$P_{e\to e}$ (%)	$P_{e\to\pi}$ (%)
0.3 - 0.4	64	8	70	10
0.4 - 0.5	64	7	65	10
0.5 - 0.7	76	4	77	6
0.7 - 0.9	87	2	84	5
0.9 - 1.1	92	1.5	87	3

an e^+e^- experiment, positive identification of pions without contamination from electrons is as often required as is electron identification free from pion contamination. The degree of discrimination possible is limited by shower fluctuations and compromised by the manner in which the shower detector is divided in shower depth to provide photon efficiency. The method of discrimination is discussed in a later section.

Calibration and Coil Correction

Calibration of the electronics consists of injecting graduated amounts of charge simultaneously into all channels in order to measure gain, offset, and rms noise channel by channel for the entire electronics chain. The electronics is calibrated three times daily, principally for diagnostic purposes since it is stable over much longer periods of time. This calibration accounts for signal losses due to ballistic deficit; however, a further channel-by-channel correction is necessary for signal losses due to the high-voltage blocking capacitors. These correction factors were determined before the lead stacks were enclosed in their cryostats. Measured charges from showers are converted channel by channel to deposited energies on-line.

Recorded deposited energies are converted off-line into incident energies using a constant (one for each detector module) to account for the fraction (12%) of shower energy sampled in the liquid argon. These module-dependent constants are determined by normalizing the observed Bhabha energy to the beam energy. They have been stable to within 2% over all running following any given detector fill.

To correct for ionization and radiation losses in the 1.36 radiation lengths of preradiator and for shower leakage out the rear of the fourteen radiation length lead stack, the true incident electron energy is parameterized as:

$$E_{true} = E_{stack} + \Delta E_{coil} + \Delta E_{leak} ,$$

where E_{stack} is the measured electron energy in the lead stack. At SPEAR energies ΔE_{leak} is a small ($\lesssim 2\%$) correction, but at higher PEP energies it will involve more complicated weighting of shower development to compensate for fluctuations in shower leakage. ΔE_{coil} is parameterized as:

$$\Delta E_{coil} = \Delta E_{ioniz} + \Delta E_{rad} + E_{tr} .$$

ΔE_{ioniz} and ΔE_{rad} (62.4 MeV and $52.0 + 72.5 \log(E/600)$ MeV respectively for normal incidence) are obtained by Monte Carlo shower simulation using EGS. E_{tr} corrects for variations in ΔE_{rad} using the measured energy in the "massless" gaps preceding the lead stack. Figure 8 shows that ΔE_{coil} is well-determined by this method.

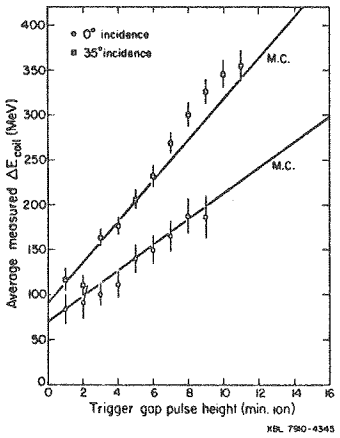

Fig. 8. Average energy loss in preradiator as a function of pulse height (measured in units of pulse height from a single minimum ionizing track) in the massless gaps. Data points are measured for 2.21 GeV Bhabha electrons. Curves are Monte-Carlo calculations.

Data points in the Figure are from a sample of Bhabha electrons and solid lines are Monte-Carlo predictions.

Correction of photon energies is similar except that (1) no ΔE_{ioniz} term is used; (2) ΔE_{rad} and E_{tr} are parameterized differently than for electrons; and, in the case of low energy photons ($E_\gamma < 300$ MeV), (3) an additional small correction is made for the effect that detection is favored for showers with fluctuations (both shower and noise) towards higher observed energies.

Shower Reconstruction

Charged particles and photons are reconstructed separately. Drift chamber tracking provides the position and direction of charged particles entering the detector, guiding reconstruction of deposited energy along the charged particle trajectory without pattern recognition. Tracking done this way is free from bias associated with the manner in which the particle deposited energy (showered, strongly interacted, ionized only, etc.). This method of charged particle reconstruction provides maximal information for electron-hadron discrimination.

For efficient photon reconstruction, even at low energies, showers with small deposited energies comparable to the level of detector noise (equivalent to approximately 8 MeV incident) must be recognized. Furthermore, low energy photons must be reconstructed without creating spurious photons from coincidences of noise fluctuations or of noise fluctuations and real deposited energy. Photon reconstruction consequently consists of several steps which compromise between the goals of high efficiency and very few accidentals. First, hits are defined by low cuts (2× rms noise) on the pulse heights in individual layers, allowing for fluctuations which reduce the energy deposit in any one layer. Then, for spatial coincidences of hits in several layers a more stringent requirement (typically about 10 MeV) on the sum of deposited energies is made, favoring real energy deposition relative to uncorrelated noise fluctuations. However, to be efficient for photons, regardless of their shower development, four different pattern recognition algorithms separately define spatial coincidences using the redundant coordinate determination afforded by seven layers of readout. Twenty-five percent more incident photons, and 67% below 200 MeV, are reconstructed by using four algorithms instead of only the single most successful algorithm. Checks on ambiguity of reconstruction and on characteristics of the shower development reduce the number of spurious photons. For some physics applications, spurious photons are also eliminated by ignoring all photons near a charged track. The probability of a spurious photon in a given event depends on event topology. For events with two charged tracks and no real photons, a spurious photon will be present in 6% of all events, as determined with cosmic ray and Bhabha events. For events with two charged tracks and two real photons, the probability of a spurious photon rises to about 13%, as determined with $e^+e^- \to \psi \to \pi^+\pi^-\pi^0$ events. Figure 9 shows the spectrum of spurious photons from cosmic ray events compared with the photon spectrum from the same number of events of the sort $e^+e^- \to$ hadrons.

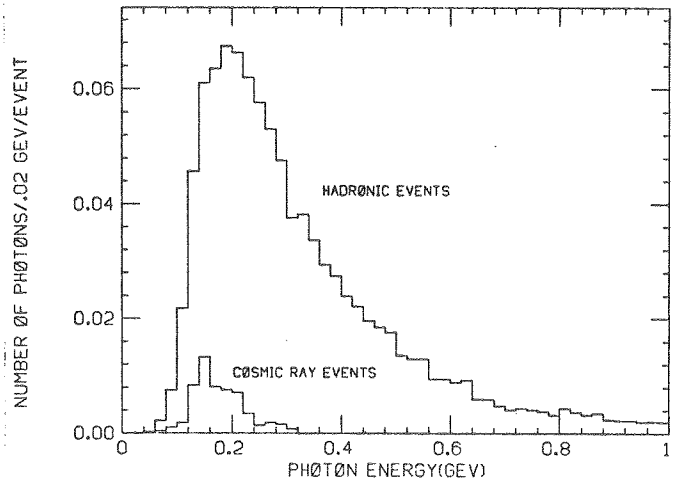

Fig. 9. Energy spectra of reconstructed photons from hadronic events and from cosmic ray events. The spectra are normalized to the same number of events. The cosmic ray spectrum represents spurious photons; whereas, the hadronic spectrum includes both real and spurious photons.

Method of Electron-Hadron Discrimination

Electron-hadron discrimination is performed using the method of "recursive partitioning for non-parametric classification".[8] In this method well-understood samples of conversion and Bhabha electrons and charged pions from the decay $\psi \to \pi^+\pi^-\pi^+\pi^-\pi^0$ are used to construct

a binary decision tree utilizing measured quantities. The quantities used include pulse heights and shower widths in each of the seven shower detector layers and a small number of combinations of the pulse heights, as well as the drift chamber measured particle momentum and scintillator determined time of flight (for particles below momenta of 500 MeV/c). The decision tree is constructed using a recursive algorithm that chooses the tree which provides the best separation between the training samples. The variables found most powerful in separating pions and electrons at SPEAR energies in our geometry are the ratio of total shower energy to momentum measured by the drift chambers, the pulse height in the massless gaps, and the ratio of total energy to the energy in the layers at the front of the detector. The method allows identification efficiency and misidentification probability to be varied according to physics requirements for particular applications. Table 1 summarizes an example of discrimination provided by a particular choice of classification.

Summary

Although the cryogenic and electronic problems of a large lead/liquid argon shower system such as in the Mark II require considerable attention to detail during design, construction, and set-up, the performance of a large system equals that of small test systems and agrees well with reasonable expectations. The shower detector system of the Mark II has been mechanically, cryogenically, and electronically very reliable during eighteen months of normal operation at SPEAR. Performance has provided a good compromise among the various demands upon shower detection. The system has enabled physics measurements previously untenable to other e^+e^- detectors.

Acknowledgements

We wish to acknowledge the contributions of our colleagues in the SLAC-LBL Mark II collaboration in helping maintain, operate, and evaluate the performance of the lead/liquid argon system. We are particularly grateful to Bob Watt, Jerry Hern, and the Cryogenics Group at SLAC for providing the technical support crucial to the operation of our large cryogenic system.

This work was supported by the Department of Energy under Contract No. DE-ACE3-765F00515 and No. W-7405-ENG-48.

References

1. W. J. Willis and V. Radeka, Nucl. Instr. and Meth. 120, 221 (1974).
2. J. H. Cobb et al., Nucl. Instr. and Meth. 158, 93 (1979).
3. G. S. Abrams et al., IEEE Trans. on Nucl. Sci. NS-25, No. 1, 309 (1978).
4. G. S. Abrams et al., The Lead/Liquid Argon Shower Counter System for the Mark II Detector, to be submitted to Nucl. Instr. and Meth.
5. E. L. Cisneros et al., IEEE Trans. on Nucl. Sci. NS-24, No. 1, 413 (1977).
6. M. Breidenbach et al., IEEE Trans. on Nucl. Sci. NS-25, No. 1, 706 (1978).
7. R. L. Ford and W. R. Nelson, EGS Code, SLAC Report No. 210 (1978).
8. J. Friedman, IEEE Trans. on Computers C26-4, 404 (1977).

TECHNICAL INFORMATION DEPARTMENT
LAWRENCE BERKELEY LABORATORY
UNIVERSITY OF CALIFORNIA
BERKELEY, CALIFORNIA 94720